SPE 63087

Guidelines for Choosing Compositional and Black-Oil Models for Volatile Oil and Gas-Condensate Reservoirs

Øivind Fevang, SPE, PERA, Kameshwar Singh, SPE, NTNU, and Curtis H. Whitson, SPE, NTNU/PERA

This paper was prepared for presentation at the 2000 SPE Annual Technical Conference and Exhibition held in Dallas, Texas, 1–4 October 2000.

Abstract

This paper provides specific guidelines for choosing the PVT model, black-oil or equation of state (EOS), for full-field reservoir simulation of volatile/near-critical oil and gas condensate fluid systems produced by depletion and/or gas injection.

In the paper we have used a "generic" reservoir from the North Sea containing a fluid system with compositional grading from a medium-rich gas condensate upstructure, through an undersaturated critical mixture at the gas-oil contact, to a volatile oil downstructure.

A component pseudoization procedure is described which involves a stepwise automated regression from the original 22-component EOS. We found that a six-component pseudoized EOS model described the reservoir fluid system with good accuracy and, for the most part, this EOS model was used in the study.

Methods are proposed for generating consistent black-oil PVT tables for this complex fluid system. The methods are based on consistent initialization and accurate in-place surface gas and surface oil volumes when compared with initialization with an EOS model. We also discuss the trade-off between accurate initialization and accurate depletion performance (oil and gas recoveries).

Each "reservoir" is simulated using black-oil and compositional models for various depletion and gas injection cases. The simulated performance for the two PVT models is compared for fluid systems ranging from a medium rich gas condensate to a critical fluid, to slightly volatile oils. The initial reservoir fluid composition is either constant with depth or exhibits a vertical compositional gradient. Scenarios both with saturated and undersaturated GOC are considered. The reservoir performance for the two PVT models is also compared for different permeability distributions.

Reservoir simulation results show that the black-oil model can be used for *all* depletion cases if the black-oil PVT data are generated properly. In most gas injection cases, the black-oil model is not recommended — with only a few exceptions.

We also show that black-oil simulations using solution oil/gas ratio equal to zero (r_s=0) does not always define a *conservative* ("P10") sensitivity for gas injection processes. If gravity segregation is strong, the incremental loss of oil recovery due to "zero vaporization" is more than offset by exaggerated density differences caused by erroneous gas densities.

Introduction

Reservoir simulation is a versatile tool for reservoir engineering. Usually CPU-time is the limiting factor when the simulation model is made. The objective of this paper is to provide guidelines for choosing black-oil or compositional reservoir simulators. The paper also recommends procedures for generation of black-oil PVT tables and for initialization of black-oil and pseudoized EOS simulation models. Furthermore, a stepwise component pseudoization procedure in order to minimize the number of component when a compositional simulator is required.

Simulated production performance both for injection and depletion from black-oil and compositional are compared for a variety of reservoir fluids ranging a medium rich gas condensate to a critical fluid, to slightly volatile. Both reservoirs with constant composition and compositional grading reservoir with depth have been simulated.

Selection of Reservoir Fluid System

A fluid sample was selected from a North Sea field. The reservoir is slightly undersaturated with an initial reservoir pressure of 490 bara at the "reference" depth of 4640 m MSL. The selected reference sample contains 8.6 mol-% C_{7+}, it has a two-stage GOR of 1100 Sm^3/Sm^3 and a dewpoint of 452 bara at 163 ^oC. **Table 1** gives the reference fluid composition **(Fig. 1)**.

22-Component SRK EOS Model

The Pedersen et al. SRK[1] EOS characterization method was used to generate the "base" EOS model. Decanes-plus was split into 9 fractions using the EOS simulation program PVTsim.

The Pedersen et al[2]. viscosity correlation is known to be more accurate in viscosity predictions than the LBC[3] correlation, particularly for oils. We therefore used the Pedersen predicted viscosities as "data" to tune the LBC correlation[4] (i.e. the critical volumes of C_{7+} fractions). To cover a range of viscosities that might be expected during a gas injection project, we also generated viscosity "data" using mixtures of the reference fluid and methane, flashing the mixtures at pressures in the range 100 to 300 bara. This resulted in oil viscosities up to 7 cp, considerably higher than reservoir oil "depletion" viscosities from the reference fluid (maximum 0.5 cp).

For gas viscosities, the difference between the tuned LBC correlation and Pedersen viscosities ranged from -5 to -12%. For oil viscosities, the tuned LBC correlation predicts oil viscosities about ±15% compared with Pedersen viscosities.

The final 22-component EOS/LBC model is given in **Table 2**.

Isothermal Gradient Calculation

Based on isothermal gradient calculations[5] using the "base" 22-component SRK EOS model the reservoir fluids vary from medium rich gas condensate to highly-volatile oil in the depth interval from 4500 to 5000 m MSL, with GORs ranging from 1515 to 244 Sm^3/Sm^3, C_{7+} content ranging from 6.9 to 22 mol-%, dewpoints ranging from 428 to 473 (maximum), and bubblepoints pressure ranging from 473 to 435 bara (**Table 3**). The reservoir pressure varies from 485 bara at the top to 509 bara at the bottom. At the GOC, reservoir pressure is 495 bara and (critical) saturation pressure is 473 bara — i.e. the reservoir is undersaturated by 22 bar at the GOC. Variations in C_{7+} and saturation pressure are shown in **Fig. 2**.

Selection of Different Fluid Samples

In this study we used different fluid systems for a given "reservoir", all originating from the compositional gradient calculation using the 22-component EOS model. The fluid systems are:

1. Compositional gradient throughout the entire reservoir, from undersaturated gas-condensate at the top to a lower-GOR volatile oil at the bottom; middle geologic unit.
2. Only the grading gas condensate fluids above the GOC (i.e. remove the underlying oil); top geologic unit.
3. Only the grading oil below the GOC (i.e. remove the overlying gas); bottom geologic unit.
4. A gas condensate, initially undersaturated, is taken from a specified depth in the reservoir. This gas condensate fluid is assumed to have constant composition with depth.
5. A relatively-low GOR volatile oil taken at a specified depth in the reservoir. This oil is assumed to have constant composition with depth.
6. A low-GOR oil was "constructed" from the oil at 250 m below the GOC, where this oil was further flashed to a pressure of 135 bara with a resulting GOR of 50 Sm^3/Sm^3.

For fluid systems (4) and (5) above, several fluids were selected at depths 250, 50 and 10 m above and below the GOC, as well as the GOC composition. In this way, seven "samples" were used from the single compositional gradient calculation (Fig. 2).

Pseudoization – Reducing Number of Components

Because it is impractical to conduct full-field and large-sector model simulations using the 22-component EOS model (due to CPU and memory limitations), several "pseudoized" or reduced-component EOS models were developed – EOS models with 19-, 12-, 10-, 9-, 6-, 4-, and 3 components.

The pseudoization procedure is summarized below:

1. Using the original (22-component) EOS model, simulate a set of PVT experiments which cover a wide range of pressures and compositions expected in the recovery processes used to produce a reservoir.
2. PVT experiments included constant composition tests, depletion-type experiments (differential liberation and constant volume depletion), separator tests, and multicontact gas injection (swelling) tests. Two quite-different injection gases (**Table 4**) were used for the swelling test simulations.
3. The simulated PVT properties were used as "data" for the step-wise pseudoizations.
4. At each step in pseudoization, new pseudocomponents were formed from existing components. Regression was used to fine tune the newly-formed pseudo-component EOS parameters and a select number of BIPs.
5. Step 4 was repeated a number of times, trying (manually) to select the best grouping at each stage in the pseudoization process.

The procedure allows the determination of which components are best to group, and at what point during pseudoization that the quality of EOS predictions deteriorate beyond what is acceptable for engineering calculations.

Generating the 22-Component EOS PVT "Data"

The 22-component EOS model was first used to generate a large set of PVT data. A total of eight feeds (one reference sample and seven generated from the compositional gradient calculation; four gas samples, one near-critical sample, and three oil samples) were used for generating PVT data. Depletion-type PVT tests and separator tests were used, together with swelling-type tests for several injection gases. All calculated PVT results using these feeds were treated as "data" for pseudoization.

A total of 8 CCE-, 8 SEP-, 5 CVD-, 8 DLE- and 8 MCV experiments were used for generating the "data" for pseudoization.

Stepwise Pseudoization

First, a 19-component EOS model was obtained after grouping C_1+N_2, i-C_4+n-C_4, and i-C_5+n-C_5.

The regression parameters for PVT fits were EOS constants A and B of the newly-formed pseudo-components and (collectively) the binary interaction parameters between C_1 and C_{7+}. All simulated tests were used for the PVT fit. For viscosity fits (at each stage in the pseudoization process), only DLE and MCV viscosity data were used in regression. Viscosity regression parameters were the critical volumes of the newly-formed pseudocomponents.

PVT properties of the 19-component EOS model matched the 22-component EOS model almost exactly.

The 12-component EOS model was obtained by grouping the original eleven C_{7+} fractions into 5 fractions on the basis of (more-or-less) equal mass fraction of the C_{7+} fractions. The heaviest component was kept as the original fraction and other C_{7+} components were grouped into 4 pseudo-components. Regression was performed again, where we found that the 12-component EOS model predicts PVT properties very similar to the 22-component EOS model.

The 10-component EOS Model was obtained after reducing C_{7+} fractions from 5 to 3 fractions based on equal mass fraction of the C_{7+} fractions. Regression was performed and the 10-component EOS model predicts PVT properties which are comparable with the 22-component EOS model.

In the 9-component EOS model, C_2 and CO_2 were grouped together. There is little change from the 10-component EOS.

Further grouping was done in steps. In each step, one component was grouped with another suitable component and properties were compared with the 22-component EOS model (after regression). From the 9-component EOS model we grouped to 8-, 7-, and finally 6 components. Based on our previous experience, it has been found that it is usually necessary to have 3 C_{7+} fractions. Our final 6-component EOS model contained 3 C_{7+} components and 3 C_{6-} components: (N_2,C_1), (CO_2,C_2), (C_3-C_6), (C_7-F2), (F3-8), F9, given in **Table 5**.

From the 6-component EOS model, another series of grouping was conducted. The 4-component EOS model contained only 2 C_{7+} fractions, where a reasonable match was obtained for most PVT properties. However, from the 4-component model to the 3-component model, PVT properties deteriorated significantly. The deviation in most of the PVT properties was large using the 3-component EOS.

The 22-component EOS model versus the 6-component EOS model PVT properties are shown in **Figs. 3** and **4.**

As an independent check on the validity of the pseudoized EOS models, we used depletion recovery factors calculated from CVD tests as a verification of how accurate the pseudoized models maintained surface oil and surface gas recoveries when compared with the original EOS22 model. CVD data are used to compute surface oil and gas recoveries[6] at different pressures (based on simplified surface flash). The difference in oil recoveries is shown in **Figs. 5** and **6**. When deviation in condensate *recovery* is used for comparison (Fig.5) the leanest upstructure gas at 4500 m shows the largest difference between EOS6 and EOS22. However, in terms of *reserves*, Fig. 6 shows that the largest error is in the richest downstructure gas at 4750 m, where a "typical" North Sea HCPV has been used to convert recovery factors to reserves.

Black-Oil PVT Properties

In the black-oil model, the PVT system consists of two reservoir phases – oil (o) and gas (g) – and two surface components – surface oil ($\bar{o}$) and surface gas ($\bar{g}$). The equilibrium calculations in a black-oil model are made using the solution gas-oil and solution oil-gas ratios R_s and r_s, respectively, where surface "component K-values" can be readily expressed in terms of R_s and r_s.

Black-oil PVT properties have been generated in this study with an EOS model using the Whitson-Torp procedure[7]. In this approach, a depletion-type experiment is simulated – either a CCE, CVD, or DLE test. At each step in the depletion test, the equilibrium oil and equilibrium gas are taken separately through a surface separation process. The surface oil and surface gas products from the reservoir oil phase are used to define the oil FVF B_o and the solution GOR R_s. The surface oil and surface gas products from the reservoir gas phase are used to define the "dry" gas FVF B_{gd} and the solution OGR r_s.

It is also necessary to choose a single set of *constant* surface gas and surface oil densities used to calculate reservoir densities (together with pressure-dependent properties R_s, B_o, r_s, and B_{gd}). Proper selection of surface "component" densities can ensure improved accuracy in black-oil reservoir density calculations.

For saturated reservoirs initially containing both reservoir oil and reservoir gas, the black-oil PVT properties may differ in the "gas cap" and "oil zone" regions. Consistent treatment of this problem may be important. The best approach is to perform a depletion test on the initial reservoir gas alone, retaining only the r_s, μ_g, and B_{gd} properties, and separately performing a depletion test on the initial reservoir oil alone, retaining only the R_s, μ_o, and B_o properties.

A special problem involves generating black-oil PVT properties for gas injection studies in an undersaturated oil reservoir. This involves extrapolation of the saturated oil PVT properties, sometimes far beyond the initial bubblepoint pressure. Several methods can be used for generating the extrapolated saturated BO PVT tables, but we have found one which seems consistently better.

Reservoir Simulation – Initialization

To obtain correct and consistent initial fluids in place (IFIP) for black-oil and compositional models it is important to initialize the models properly. This involves proper treatment of (1) fluid contacts and phase definitions, (2) PVT models, (3) compositional (solution-GOR) gradients, and (4) the

relative importance of IFIP versus ultimate recoveries for the relevant recovery mechanisms.

Initializing EOS Models

The reservoir was initialized with the 6-component EOS model[8] and initial fluids in place were compared with that of the 22-component EOS model. Three different initialization methods with the 6-component EOS model were used:

1. Method A – starting with the reference feed, the 6-component EOS model was used to make an isothermal gradient calculation, providing a compositional gradient based on the 6-component EOS model. In this method, the calculated GOC was somewhat different than with the 22-component EOS model.
2. Method B – starting with the reference feed, use the 6-component EOS model for isothermal gradient calculation and adjust the reservoir pressure at the reference depth such that the calculated GOC equaled the GOC from the 22-component model. The resulting compositional gradient using the 6-component EOS model was then used in the reservoir simulation model, but with the correct reservoir pressure at reference depth.
3. Method C - use the 22-component EOS model for the gradient calculation, and then manually pseudoize to obtain the 6-component compositional gradient.

The C_{7+} compositional variation with depth for the above three methods is shown in **Fig. 7**. Method C gives the most correct reservoir fluid compositional gradient (when compared with the 22-component initialization). The initial fluids in place calculated with the different methods are given in **Table 6**.

Method C is recommended *in general* for initializing pseudoized EOS models. This assumes, however, that the saturation pressure gradient and key PVT properties are similar for the full-EOS and pseudoized-EOS models; differences in saturation pressures (**Fig. 8**) and PVT properties will potentially have an impact on recoveries. With our pseudoization procedure these differences were minimized and make method C the recommended procedure.

Initializing Black-Oil Models

For obtaining accurate initial fluids in place and description of reservoir recovery processes, black-oil PVT tables and "compositional gradients" must be selected carefully.

The compositional gradient in a black-oil model is given by the depth variation of solution GOR (R_s) in the oil zone and the solution OGR (r_s) in the gas zone. The use of solution GOR and OGR versus depth – *instead of saturation pressure versus depth* – is important for minimizing "errors" in initial fluids in place.

The choice of how to generate a *proper* black-oil PVT table includes the following issues:

1. Whether the purpose is (a) to describe accurately the actual reservoir PVT behavior or (b) for the purpose of comparing black-oil with compositional simulation results.
2. Treatment of compositional gradients, and whether the reservoir has a saturated gas-oil contact or an undersaturated "critical" gas-oil contact.
3. Extrapolation of saturated PVT properties to pressures higher than the maximum saturation pressure found initially in the reservoir.
4. Choice of the surface gas and surface oil densities to minimize the "errors" in reservoir gas and reservoir oil densities calculated from the black-oil PVT tables — used to compute the vertical flow potential for (a) static initialization and (b) dynamic flow calculations.

In this study a single reference fluid had been obtained by sampling in the gas cap. This sample, based on the isothermal gradient calculation with the EOS22 and EOS6 models, indicated a fluid system with compositional grading through a critical (undersaturated) gas-oil contact.

It was necessary to extrapolate the black-oil PVT properties at least to the maximum saturation pressure of the critical mixture at the gas-oil contact. Three methods of extrapolation were studied, all based on the EOS6 model:

1. Adding incipient (oil) phase composition to the reference sample until the saturation pressure reached the GOC saturation pressure.
2. Adding the GOC composition from the gradient calculation to the reference sample until the saturation pressure reached the GOC maximum value.
3. Using the GOC composition itself.

For each method, a composition with a saturation pressure equal to the GOC critical fluid saturation pressure was obtained. This composition was then used to generate the black-oil PVT tables using a constant composition expansion experiment (with separator tests conducted separately for each equilibrium phase during the depletion).

To initialize the black-oil model[9], we first chose a solution GOR&OGR versus depth relation. From the discussions in the previous section, Methods A, B, and C were used for generating compositional variation with depth for the 6-component EOS model. From the compositional gradient with depth, each of the three methods also generated a solution GOR&OGR versus depth relation. When comparing black-oil initialization using the three methods A, B, and C combined with the three methods for generating black-oil PVT properties (1, 2, and 3 above), we found that Method C always gave more accurate and consistent initial fluids in place; by consistent we mean that the method provided a more accurate estimation of the 22-component EOS initialization. The most accurate and consistent IFIP in the black-oil model was achieved using Method C for solution GOR versus depth together with Method 3 for generating the black-oil PVT tables.

The comparative (EOS22 vs. EOS6 and EOS6 vs. BO6) initial fluids in place are given in Table 6.

The most important aspect of initializing a black-oil model for a reservoir with compositional gradients is the proper use of solution OGR and solution GOR versus depth. These two

black-oil PVT properties represent in fact *composition* and should, accordingly, be used to initialize the reservoir model. It would not make sense, for example, to initialize a compositional simulator with saturation pressure versus depth, and it is equally "illogical" in a black-oil model – with the added disadvantage that the resulting initial fluids in place can be very wrong.

Because a single PVT table is often used in a black-oil model, and particularly for reservoirs with an undersaturated critical GOC, we know that the resulting PVT pressure dependence of fluids throughout the column are not represented exactly. Fluid at each depth has its "own" set of black-oil PVT tables — i.e. the pressure dependence of PVT properties is somewhat different for fluids at different depths. This is shown in **Figs. 9** and **10**. Initializing with solution GOR versus depth is accurate because the variation in oil formation volume factor with solution gas-oil ratio is similar for the different fluids, as shown in **Fig. 11**.

Despite an initialization of composition with depth in a black-oil model, where solution OGR and solution GOR are taken directly from the compositional EOS model, we know that the saturation pressure versus depth will not be represented properly in the black-oil model. This "error" in saturation pressure versus depth has practically no effect on initial fluids in place, but it does have a potential effect on depletion recoveries. Figs. 9 and 10 show the magnitude of error in saturation pressure found in the black-oil model initialized based on correct solution OGR and solution GOR versus depth.

Our experience shows that the error in saturation pressure versus depth usually has little impact on production performance and ultimate recoveries. It may have a short-lived effect on recovery (rates) versus time as the reservoir depletes below the initial saturation pressures; ultimate recoveries are not usually affected noticeably.

Reservoir Simulation Examples

Basic Reservoir and Model Data. The basic reservoir and fluid properties are given in **Table 7**. The relative permeabilities are shown in **Fig. 12**.

The generic reservoir simulation model contains three geological units. The thickness of each unit is 50 meters. Each geological unit generally has ten numerical layers and each layer has a constant permeability. The heterogeneity of each geological unit is described by a Dykstra-Parsons coefficient of 0.75. The average permeability in each geological unit is 5, 50, and 200 md (top, middle and bottom). The reservoir has a dip of 3.8 degrees.

The base numerical model for one geological unit has 50x10x10 grid cells. The base case has a vertical producer, which is located downdip in cell (50,10) and is perforated in all layers. The producer is controlled by a reservoir volume rate of 10% hydrocarbon pore volume per year.

Nomenclature and a short description of all the simulation cases discussed in this paper are given in **Table 8** and **9.**

Full EOS versus Pseudoized EOS

Simulation cases with depletion and with gas injection were simulated with the full 22-component and the 6-component fluid characterization to verify that the 6-component characterization accurately describes production performance. The near-critical fluid with constant composition was selected for depletion performance. The depletion performance of the two EOS models are very similar as shown in **Figs. 13** and **14**. We selected the near-critical fluid with lean gas injection for the injection case. The production performance was very close, as shown in **Figs**. **15** and **16.** We have used 6-component EOS model for all subsequent simulation cases.

BOvsEOS Reservoir Simulation — Depletion

This section compares simulation results from a black-oil model with a compositional model[10-13] for different depletion cases. Simulated production performance for the two models are compared for fluid systems ranging from a medium rich gas condensate, to a critical fluid, to slightly volatile oils. The initial reservoir fluid composition is either constant with depth or shows a vertical compositional gradient. Scenarios both with saturated and undersaturated GOC are studied. Permeability increases downwards in most cases to maximize the effect of gravity and mixing of the reservoir fluids. Sensitivities have also been run with different permeability distributions.

Table 8 gives a summary of the performance of all the depletion cases we ran in this study. Only a few of the simulation cases are discussed here (marked in bold). Data sets for all cases are available upon request.

The simulated field oil production from black-oil model runs did not deviate more than one recovery-% from the compositional results during the ten-year production period in any case. In most cases the deviation was less then 0.25 recovery-%. The difference in gas recovery was negligible in all cases. The producing GOR is generally quite accurate during most of the ten-year production period. However, in a few cases, the producing GOR started to deviate somewhat after about five years of production and after ten years of production the GOR was up to 10% lower in the black-oil model. It should be noted that in the case of a reservoir with a large compositional gradient, the producers high on the structure will generally have a producing GOR in the black-oil model somewhat (5-10%) too low. However, if the main part of the oil production comes from downdip wells then the overall field oil production will be accurately predicted by the black-oil model.

Reservoirs with an Undersaturated GOC. The black-oil PVT tables should be generated by simulating a CCE experiment using the critical GOC fluid. In Eclipse 100, the black-oil PVT table needs to be manually extrapolated to a saturation pressure higher than the initial reservoir pressure at GOC.

Black-oil PVT data for fluids with a saturation pressure 30-50 bar from the critical point may cause convergence problems. This is due to the highly non-linear PVT behavior near the critical point. Fortunately, these near-critical data can be deleted from the black-oil PVT tables without changing the production performance.

In this paper we show the production performance for three different cases:

1. A near-critical fluid with constant composition (**Figs. 17** and **18)**.
2. A near-critical fluid with compositional gradient (**Figs. 19** and **20)**.
3. Volatile oil with constant composition with highest permeability at the top **(Figs. 21** and **22)**.

Reservoirs with a Saturated GOC. In the following cases the black-oil PVT tables have been generated from a simulated DLE experiment with the GOC oil for the reservoir oil. The reservoir gas PVT table has been generated from a simulated CVD experiment with the GOC gas. When significant gravity segregation is expected, the surface-gas and surface-oil densities should be modified such that the reservoir-oil and reservoir-gas densities are accurate throughout depletion.

The simulated field production performance was very similar for both models for all the cases shown in Table 8.

Only one simulation case showed some difference between the black-oil and the compositional model. In this case, there were three wells completed at different locations structurally - high, middle and low. All the wells were completed throughout the reservoir (i.e. 10 numerical layers). For the structurally high wells the performance was different in the two models (**Figs**. **23** and **24**). The structurally-high well produced with a too-low GOR below the "saturation pressure" in the black-oil simulation compared to the compositional model. The difference in producing GOR is due to an error in saturation pressures in the black-oil simulation as discussed earlier and demonstrated in Fig. 9. Even though the individual wells showed some performance differences, the overall 3-well total performance is very similar as shown in **Figs. 25** and **26**.

BOvsEOS Reservoir Simulation — Gas Injection

This section compares simulation results between an EOS simulator and a black-oil simulator for many cases with gas injection. We have tried to examine if any general guidelines can be found when a black-oil model can be used to simulate gas injection. We found it difficult to come up with general rules, though some guidelines are given. Summaries with "key" production data for all of the simulation runs are reported in **Table 9**. A few cases are discussed below.

Full Pressure Maintenance

Gas Condensate Reservoirs with Constant Composition. For gas cycling in gas condensate reservoirs above the dew point, Coats[10] showed that black-oil simulators can be used. **Figs. 27** and **28** show the performance of a reservoir with a medium rich gas condensate with constant composition. The oil recovery after 15 years of production is 82.4% in the compositional model and 84.2% in black-oil model. Note the effect of gravity in this case is small.

Most of our simulation results support the conclusion by Coats[10] that gas condensate reservoirs produced by gas cycling above the original dewpoint can be simulated accurately with a black-oil simulator.

However, we found in some cases with (1) a rich gas condensate and (2) increasing permeability downwards, that a black-oil simulator significantly overpredicts oil recovery due to compositional effects that are not properly treated in a black-oil model. This is shown in **Figs. 29** and **30**, where oil recovery after 15 years is 71.3% in the compositional model and 88.7% in the black-oil model; the difference in oil recovery is less for high permeability at the top (50% versus 56% oil recovery).

A black-oil simulator may be adequate in reservoirs where the displacement process is gravity stable or where the effect of gravity is negligible.

Oil Reservoir with Constant Composition. A black-oil model may over-predict oil production for high-pressure gas injection because oil vaporization is over-estimated. Lean gas injection in reservoirs with some swelling but with minor vaporization effects can in most cases be simulated with a black-oil simulator if the black-oil PVT tables are generated using the guidelines outlined below.

Black-oil PVT tables used in injection processes are made by splicing the black-oil PVT tables for the original reservoir oil and the swollen oil. Black-oil PVT data for the swollen oil is generated using a multi-contact swelling experiment. The injection gas is added to the original oil sample in steps until the saturation pressure of the swollen oil is somewhat higher than the maximum (injection) pressure.

The modified black-oil PVT tables (both oil and gas) used in the simulation model can be generated using three different approaches:

A. Original BO PVT table + incremental swollen oil properties from the original bubblepoint to the highest pressure.
B. Original PVT table + depletion of the fully-swollen oil to the saturation pressure of the original oil.
C. Original PVT table + one additional data at the fully-swollen saturation point.

The modified black-oil PVT data for the different approaches are shown in **Figs. 31** through **34** for lean gas injection into a slightly volatile oil.

The reservoir performance for a near-saturated low-pressure reservoir (P_R= 200 bara and P_b= 135 bara) with low-GOR oil is shown in **Figs. 35** and **36**. The difference in cumulative oil production between method B and the compositional model is less than 2 recovery-% during simulation period (20 years). However the black-oil model under predicts the producing GOR at high producing GORs for all methods. The difference between the three methods are

generally small as shown in this case. However, based on experience method B seems to be consistently better.

For highly-undersaturated low-GOR oils a black-oil model does not accurately describe the production performance as shown in **Figs. 37** and **38.** In this case the same low-GOR oil as in the previous case was used but the initial reservoir pressure was increased to 500 bara.

In Figs. 37 and 38, the performance is also shown for a case with swelling but without vaporization, and a case with no vaporization and no swelling. The black-oil simulation case with swelling but without vaporization has a higher oil recovery the first 15 years than the compositional model. The oil production rate in the period 3-5 years after start of production is up to 50% higher in the black-oil model without swelling compared to the compositional model. The reason for this is that the loss of oil recovery for "zero vaporization" is more than offset by exaggerated gravity effects caused by too-low gas densities; $\Delta\rho_{og}$ is too high.

The production performance is also compared for black-oil and compositional simulations for a slightly volatile oil. The black-oil PVT properties for the slightly volatile oil are shown in Figs. 31 through 34. The simulated production performance curves are shown in **Figs. 39** and **40.** In this case the black-oil simulation run with swelling but with no vaporization and the black-oil simulation with no swelling and with no vaporization are quite similar, but quite different from the compositional model. The oil plateau production period is 1.5 years in the compositional model and about 3 years in the black-oil models with no vaporization with/without swelling. The black-oil simulation run with vaporization and swelling using method B is quite close to the compositional model the first 5 years of production. After 5 years the oil production is over predicted. For this case the results from the black-oil model (with swelling and vaporization) were about the same, independent on the different methods used to generate the modified black-oil tables (Table 9).

Reservoirs with Compositional Gradient and Undersaturated GOC. In some cases, reservoirs with gas injection in the gas cap can be simulated with a black-oil simulator, particularly if the injectors are placed far above the original GOC. An example is the reservoir performance for a reservoir with compositional grading and an undersaturated GOC is shown in **Figs. 41** and **42**. In this situation, the gas-gas displacement will be miscible (if the reservoir gas near the injector is not very rich). Furthermore, the reservoir oil will be displaced miscibly by the reservoir gas since the GOC is undersaturated. However, in most cases, oil production after gas breakthrough will be too high in the black-oil model.

Partial Pressure Maintenance

Undersaturated Oil Reservoir. Various amounts of the produced gas have been reinjected into the top of the reservoir to simulate varying degrees of partial pressure maintenance (Table 9). A volatile oil reservoir has been used for all cases. The conclusion is that the black-oil model consistently over predicts oil production due to excess vaporization.

Oil Reservoir with Gas Injection in the Gas Cap. The reservoir with compositional grading has been simulated with various amounts of produced gas being reinjected (Table 9) in the gas cap. The black-oil simulator over-predicts cumulative oil production by more than 14% (6.5 recovery-%) when 100% of the produced gas is reinjected. The performance plots are shown in **Figs. 43** and **44**. Note that for full pressure maintenance, the displacement is miscible and the two simulators are much closer (Figs. 41 and 42).

Recommended Procedures

Black-Oil PVT Properties — Depletion

Independent of the type of reservoir fluid, we have found that it is important to include undersaturated properties for fluids with different saturation pressures – not only the fluid with the highest saturation pressure.

Whether the black-oil PVT tables should be calculated using the full- or the pseudoized EOS depends on the purpose of the black-oil simulation. When the purpose is to compare black-oil with compositional simulation results we recommend generating the black-oil PVT tables with the same EOS model used for the compositional simulations. If accuracy in PVT is desired, black-oil properties should be generated with the full EOS. If the procedures outlined in this paper are used to pseudoize, the difference in inplace volumes between the full- and the pseudoized EOS should be small (<1% of IFIP).

Undersaturated Oil Reservoirs. For undersaturated oil reservoirs, the black-oil PVT tables are made by simulating a CCE experiment using the fluid with the highest solution GOR. Make sure undersaturated PVT properties are calculated up to maximum initial reservoir pressure; at least for Eclipse 100.

Undersaturated Gas Reservoirs. For undersaturated gas reservoirs, the black-oil PVT tables are made by simulating a CCE experiment using the fluid with the highest solution OGR. Make sure undersaturated PVT properties are calculated up to maximum initial reservoir pressure.

Saturated GOC. For reservoirs with a saturated GOC, the black-oil gas PVT table is made simulating a CVD experiment with the GOC equilibrium gas. The oil PVT table is made by simulating a DLE experiment with the GOC equilibrium oil. It is also necessary to choose a single set of constant surface gas and surface oil densities used to calculate reservoir densities (together with R_s, B_o, r_s, and B_{gd}). We recommend using surface oil and surface gas densities which give correct reservoir oil and reservoir gas densities at the GOC. The equations to calculate surface oil and gas densities are:

$$\rho_{os} = \frac{\rho_{oR}B_o - R_s\rho_{gR}B_{gd}}{1 - r_sR_s} \quad \text{.....(1)}$$

$$\rho_{gs} = \frac{\rho_{gR}B_{gd} - r_s\rho_{oR}B_o}{1 - r_sR_s} \quad \text{.....(2)}$$

Undersaturated GOC. For reservoirs with an undersaturated GOC the black-oil PVT tables are made by simulating a CCE experiment with the GOC critical fluid. Some of the nearest-to-critical-pressure data may need to be omitted if $|d(R_s)/dp|$ or $|d(r_s)/dp|$ is too large.

For reservoir simulators that do not support an undersaturated GOC, a "fictitious" saturated GOC has to be introduced. This requires using a "fictitious" saturation pressure for the critical fluid that is slightly higher than the initial reservoir pressure at the undersaturated GOC. Changing the saturation pressure of the fluids near the undersaturated GOC the second pressure point with saturated properties should be at a pressure just slightly (0.1-1.0 bar) lower than the saturation pressure of the critical fluid.

Black-Oil PVT Properties — Gas-Injection. For undersaturated oil reservoirs undergoing gas injection the injection pressure will be higher than the saturation pressure of the highest-bubblepoint oil in the reservoir. In such cases the black-oil PVT table has to be extended to include saturated oil and gas properties up to maximum pressure in the reservoir during gas injection (usually this is the maximum injection pressure). The black-oil PVT data for the swollen oil and equilibrium gas should be generated using a single-point swelling experiment. The injection gas is added to the highest-original-bubblepoint reservoir oil sample until the saturation pressure is somewhat higher than the maximum injection/reservoir pressure. The fully-swollen oil is depleted in several steps using a CCE test down to the highest-original-bubblepoint. The black-oil PVT properties from the swollen oil are then "spliced" to the PVT tables from the original oil. This procedure has always been the most accurate.

Initializing EOS Models. In most cases a full-field reservoir model uses an EOS with a reduced number of components compared to the EOS model used to develop the initial fluid characterization. The most accurate method to initialize a reservoir in such a case is to manually pseudoize the gradient calculated with the full EOS to obtain the component compositional gradient for the reduced EOS. This assumes, however, that the saturation pressure gradient and key PVT properties are similar for the full-EOS and pseudoized-EOS models.

Initializing Black-Oil Models. The compositional gradient in a black-oil model is given by variation of solution GOR (R_s) in the oil zone and the solution OGR (r_s) in the gas zone. This will lead to consistent inplace oil and gas volumes, but may result in an error in the saturation pressure versus depth. Whether the gradient should be calculated using the full or reduced EOS depends on the purpose of the black-oil simulation.

Conclusions

1. A black-oil model is always adequate for simulating depletion performance of petroleum reservoirs if (a) solution GOR and solution OGR are initialized properly, and (b) the PVT data are generated properly.
2. A compositional simulation model is generally recommended for gas injection studies. For gas injection, a black-oil model can only be used in (a) oil reservoirs when there is minimal vaporization and (b) lean to medium-rich gas condensate reservoirs undergoing cycling above the dewpoint for gas condensate fluids.
3. Initial fluids in place can be calculated accurately for pseudoized-EOS and black-oil models by initializing with the correct compositional gradient. In a compositional model, compositional gradient should be calculated from the original EOS model – i.e. the EOS model prior to pseudoization. In a black-oil model, the solution GORs and OGRs versus depth should be used. Black-oil PVT data should be generated from a properly-selected fluid with sufficiently-high saturation pressure.
4. For developing an EOS model for a reservoir fluid, C_{7+} (or C_{10+}) fraction should be split into 3-5 fractions initially. Usually, however, the EOS can be pseudoized down to as few as 6 to 8 components. When pseudoizing, key component properties are adjusted to minimize the difference between the pseudoized EOS and the original EOS for a wide range of PVT conditions and compositions.

Nomenclature

B_{gd} = dry-gas FVF, m^3/Sm^3
B_o = oil FVF, m^3/Sm^3
GOR = gas-oil ratio, Sm^3/Sm^3
OGR = oil-gas ratio, Sm^3/Sm^3
P_b = bubblepoint pressure, bara
P_d = dewpoint pressure, bara
P_R = reservoir pressure, bara
R_s = solution gas-oil ratio, Sm^3/Sm^3
r_s = solution oil-gas ratio, Sm^3/Sm^3
ρ_{gR} = reservoir gas density, kg/m^3
ρ_{gs} = surface gas density , kg/m^3
ρ_{oR} = reservoir oil density , kg/m^3
ρ_{os} = surface oil density, kg/m^3
μ_o = oil viscosity, cp
μ_g = gas viscosity, cp

Acknowledgements

We want to thank the participants of the "Guidelines for Choosing Compositional and Black-Oil Models for Volatile Oil and Gas-Condensate Reservoirs" project – Den norske stats oljeselskap a.s, Elf Petroleum Norge A/S, Mobil Exploration Norway Inc., Neste Petroleum A/S, Norsk Hydro Produksjon a.s, Norske Conoco AS, and Norwegian Petroleum Directorate (NPD) – for financial and technical support during this work.

References

1. Soave, G.: "Equilibrium Constants for a Modified Redlich-Kwong Equation of State," Chem. Eng. Sci.(1972), 27, 1197-1203.
2. Pedersen, K. S. and Fredenslund, A.: "An Improved Corresponding States Model for the Prediction of Oil and Gas Viscosities and Thermal Conductivities," Chem. Eng. Sci., 42, (1987), 182.
3. Lohrenz, J., Bray, B. G., and Clark, C. R.: "Calculating Viscosities of Reservoir Fluids From Their Compositions," J. Pet. Tech. (Oct. 1964) 1171-1176; Trans., AIME, 231.
4. Whitson C.H : "PVTx : An Equation-of-State Based Program for Simulating & Matching PVT Experiments with Multiparameter Nonlinear Regression," Version 98.
5. Whitson, C. H. and Belery, P.: "Compositional Gradients in Petroleum Reservoirs," paper SPE 28000 presented at the University of Tulsa/SPE Centennial Petroleum Engineering Symposium held in Tulsa, OK August 29-31, 1994.
6. Whitson, C.H., Fevang, Ø., and Yang, T.: "Gas Condensate PVT – What's Really Important and Why?," paper presented at the IBC Conference "Optimization of Gas Condensate Fields", London, 28-29 January 1999
7. Whitson, C. H. and Torp, S. B.: "Evaluating Constant Volume Depletion Data," JPT (March, 1983) 610; Trans AIME, 275.
8. Eclipse 300, 1998a Release
9. Eclipse 100, 1998a Release
10. Coats, K. H.: "Simulation of Gas Condensate Reservoir Performance," JPT (Oct. 1985) 1870.
11. Coats, K. H., Thomas, L. K., and Pierson, R. G.: "Compositional and Black-oil Reservoir Simulation," paper SPE 29111 presented at the 13th SPE Symposium on Reservoir Simulation held in San Antonio, TXD, USA, 12-15 February 1995.
12. Fevang, Ø. and Whitson, C. H.: "Modeling Gas Condensate Well Deliverability," SPE Reservoir Engineering, (Nov. 1996) 221.
13. El-Banbi, A.H., Forrest, J.K., Fan, L., and McCain, Jr., W.D.: "Producing Rich-Gas-Condensate Reservoirs — Case History and Comparison Between Compositional and Modified Black-Oil Approaches," paper SPE 58955 presented at the 2000 SPE International Petroleum Conference and Exhibition, Feb. 1-3.

Table 1 — Reference Fluid Composition, 4640 m MSL

Component	Mol-%	Molecular Weight	Specific Gravity
N_2	0.20		
CO_2	6.02		
C_1	67.24		
C_2	9.58		
C_3	4.39		
i-C_4	0.75		
n-C_4	1.41		
i-C_5	0.50		
n-C_5	0.55		
C_6	0.78		
C_7	1.42	90.73	0.7440
C_8	1.63	102.66	0.7740
C_9	1.00	116.79	0.7960
C_{10+}	4.53	245.96	0.8520
C_{7+}	8.58	178.00	0.8330

Table 2 — Parameters for the 22-Component SRK EOS

Component	MW M	Critical Temperature T_C K	Critical Pressure P_C bara	Acentric Factor ω	Critical Volume V_C m^3/kmol	Boiling Point T_b K
N_2	28.0	126.2	33.9	0.04	0.0898	77.4
CO_2	44.0	304.2	73.8	0.23	0.0940	194.7
C_1	16.0	190.6	46.0	0.01	0.0990	111.6
C_2	30.1	305.4	48.8	0.10	0.1480	184.6
C_3	44.1	369.8	42.5	0.15	0.2030	231.1
i-C_4	58.1	408.1	36.5	0.18	0.2630	261.4
n-C_4	58.1	425.2	38.0	0.19	0.2550	272.7
i-C_5	72.2	460.4	33.8	0.23	0.3060	301.0
n-C_5	72.2	469.6	33.7	0.25	0.3040	309.2
C_6	86.2	507.4	29.7	0.30	0.3700	341.9
C_7	90.7	528.0	34.9	0.45	0.4455	365.1
C_8	102.7	551.1	32.1	0.49	0.4576	389.9
C_9	116.8	574.2	28.9	0.53	0.4925	415.4
F1	140.1	604.7	24.1	0.59	0.5855	449.6
F2	167.6	636.3	20.7	0.67	0.6966	490.8
F3	197.5	666.9	18.4	0.75	0.8240	529.1
F4	235.5	702.1	16.4	0.84	0.9925	571.1
F5	268.6	730.2	15.4	0.92	1.1389	604.3
F6	309.3	762.9	14.4	1.01	1.3292	640.6
F7	364.4	803.8	13.6	1.11	1.5892	685.2
F8	442.4	858.4	12.8	1.23	1.9747	735.6
F9	621.6	979.3	12.1	1.32	2.9611	829.6

Component	Specific Gravity γ	Volume Shift s	BIPS k_{N2-i}	BIPS k_{CO2-i}	Parachor P
N_2	0.4700	-0.008			41
CO_2	0.5072	0.083	0.000		70
C_1	0.3300	0.023	0.020	0.120	77
C_2	0.4500	0.060	0.060	0.120	108
C_3	0.5077	0.082	0.080	0.120	150
i-C_4	0.5631	0.083	0.080	0.120	182
n-C_4	0.5844	0.097	0.080	0.120	192
i-C_5	0.6247	0.102	0.080	0.120	225
n-C_5	0.6310	0.121	0.080	0.120	233
C_6	0.6643	0.147	0.080	0.120	271
C_7	0.7440	0.044	0.080	0.100	313
C_8	0.7740	0.075	0.080	0.100	352
C_9	0.7960	0.106	0.080	0.100	392
F1	0.8071	0.150	0.080	0.100	421
F2	0.8198	0.171	0.080	0.100	491
F3	0.8306	0.174	0.080	0.100	564
F4	0.8421	0.162	0.080	0.100	650
F5	0.8522	0.142	0.080	0.100	720
F6	0.8623	0.114	0.080	0.100	800
F7	0.8743	0.069	0.080	0.100	896
F8	0.8883	0.005	0.080	0.100	1010
F9	0.9136	-0.134	0.080	0.100	1169

Table 3 — Molar Compositions from Different Depths Based on Isothermal Gradient Calculation

Component	Depth (m MSL) 4500	4640	4700	4740	4750	4760	4800	5000
N_2	0.21	0.20	0.19	0.18	0.17	0.17	0.16	0.14
CO_2	6.03	6.02	5.98	5.90	5.86	5.82	5.72	5.52
C_1	69.36	67.24	65.42	62.86	61.94	61.06	58.71	53.94
C_2	9.53	9.58	9.59	9.56	9.54	9.51	9.40	9.06
C_3	4.26	4.39	4.48	4.56	4.59	4.60	4.62	4.57
i-C_4	0.72	0.75	0.77	0.80	0.81	0.81	0.82	0.82
n-C_4	1.33	1.41	1.47	1.53	1.55	1.56	1.59	1.62
i-C_5	0.46	0.50	0.53	0.56	0.57	0.57	0.59	0.61
n-C_5	0.51	0.55	0.58	0.62	0.63	0.64	0.66	0.68
C_6	0.71	0.78	0.84	0.90	0.92	0.94	0.98	1.03
C_7	1.26	1.42	1.55	1.72	1.77	1.82	1.95	2.15
C_8	1.42	1.63	1.80	2.03	2.10	2.17	2.34	2.62
C_9	0.86	1.00	1.12	1.28	1.33	1.38	1.50	1.71
C_{10+}	3.35	4.53	5.69	7.52	8.23	8.94	10.95	15.54
C_{7+}	6.89	8.58	10.16	12.54	13.44	14.32	16.75	22.02
GOR, Sm^3/Sm^3	1515	1101	857	621	557	504	391	244
P_s, bara	428.2	452.5	465.5	473.3	473.4	472.5	465.2	434.7

Table 4 — Composition of Injection Gas, mol-%

Component	MW	Rich gas	Lean gas
N_2	28.01	0.22048	0.49000
CO_2	44.01	6.74831	0.70000
C_1	16.04	76.09282	84.11000
C_2	30.07	10.19108	8.95000
C_3	44.10	3.99573	3.66000
i-C_4	58.12	0.57026	0.53000
n-C_4	58.12	0.96544	0.85000
i-C_5	72.15	0.25467	0.21000
n-C_5	72.15	0.25128	0.19000
C_6	86.18	0.22000	0.13000
C_{7+}	90.73	0.48993	0.18000

Table 5 — Parameters for the 6-Component SRK EOS

Component	MW M	Critical Temperature T_C K	Critical Pressure P_C bara	Acentric Factor ω	Critical Volume V_C m^3/kmol	Boiling Point T_b K	
C_1N_2	16.1	190.3	45.9	0.01	0.0990	111.4	
CO_2C_2	35.4	304.8	60.8	0.16	0.1208	189.4	
C_{3-6}	55.1	418.9	37.8	0.20	0.2601	269.6	
C_{7-9}F1-2	116.9	577.4	28.4	0.54	0.5117	420.4	
F3-8	281.0	753.3	15.2	0.97	1.1163	626.7	
F9	621.6	979.3	12.1	1.32	2.5673	829.6	
Component	**Specific Gravity γ**	**Volume Shift s**	**BIPS k_{C1N2-I}**	**BIPS $k_{CO2C2-I}$**	**OmegaA Ω_a**	**OmegaB Ω_b**	**Parachor P**
C_1N_2	0.3305	0.023			0.4269	0.09	77
CO_2C_2	0.4757	0.067	0.05735		0.4440	0.0915	93
C_{3-6}	0.5630	0.099	0.00041	0.05749	0.4208	0.0837	181
C_{7-9}F1-2	0.7864	0.109	0.00027	0.04791	0.4225	0.0894	379
F3-8	0.8576	0.118	0.00027	0.04791	0.4141	0.0827	732
F9	0.9136	-0.134	0.00027	0.04791	0.4275	0.0866	1169

Table 6 — Reservoir Initialization Procedures Summary

Compositional Model				
CASE	IOIP (10^6 Sm^3)	IGIP (10^9 Sm^3)	ΔIOIP[(a)] (%)	ΔIGIP[(a)] (%)
EOS22	13.22	11.02	-	-
EOS6, Method A	13.34	11.03	0.94	0.07
EOS6, Method B	12.96	11.13	-1.98	1.00
EOS6, Method C	13.10	11.08	-0.88	0.56
Black-Oil Model				
CASE	IOIP (10^6 Sm^3)	IGIP (10^9 Sm^3)	ΔIOIP[(b)] (%)	ΔIGIP[(b)] (%)
BO6, Method 1	12.96	11.17	-1.07	0.81
BO6, Method 2	12.89	11.17	-1.60	0.81
BO6, Method 3	13.02	11.13	-0.61	0.45

(a) Deviations relation to EOS22 values
(b) Deviation relation to EOS6, Method C values

Table 7 — Reservoir and Rock Properties

Absolute Horizontal permeability, md	5 - 200
Top geologic unit, md	5
Middle geologic unit, md	50
Bottom geologic unit, md	200
Vertical/Horizontal permeability ratio	0.1
Dykstra-Parsons coefficient	0.75
Porosity, %	15
Reservoir Height, m (3 units, 50 m each)	150
Rock Compressibility, bar^{-1}	4.00E-5
Irreducible Water Saturation, %	26
Initial Reservoir Pressure, bara at 4750 m	494.68
Initial Reservoir Temperature, °C	163
Initial Gas-Oil Contact, m	4750
Critical Gas Saturation, %	2.0
Critical Oil Saturation, %	22.7
Residual Oil Saturation, %	21.5

Table 8 — Simulation Cases and Performance — Depletion

Case Name	File Name	Case Description	Model	Reservoir Performance								
				AFTER 3 YEARS			AFTER 5 YEARS			AFTER 10 YEARS		
				FOPR	FGOR	RF_o	FOPR	FGOR	RF_o	FOPR	FGOR	RF_o
				Sm^3/d	Sm^3/Sm^3	%	Sm^3/d	Sm^3/Sm^3	%	Sm^3/d	Sm^3/Sm^3	%
D1	A1C1X	Near Critical Fluid ($V_{ro\,max}$ =55%), EOS 6	EOS6	495	1674	17.9	264	2448	22.5	14	4134	26.9
	A1C3X	Near Critical Fluid ($V_{ro\,max}$ =55%), EOS 22	EOS22	505	1626	17.8	284	2243	22.5	8	5514	26.9
D2	A1C4X	Near Critical Fluid ($V_{ro\,max}$ =55%), EOS 3	EOS3	343	2646	16.3	161	4362	19.3	43	7450	22.1
Initial Fluid, Constant												
D3	A1C1X	Near Critical Fluid ($V_{ro\,max}$ =55%)	EOS6	495	1674	17.9	264	2448	22.5	14	4134	26.9
	A1C1		BO6	500	1657	17.6	274	2352	22.3	27	3723	26.8
D4	D2	Rich Gas Condensate ($V_{ro\,max}$ = 28% and r_s = 0.00115 Sm^3/Sm^3)	EOS6	328	2723	17.4	182	3844	21.5	71	5283	26.3
	D2X		BO6	329	2713	17.3	185	3772	21.5	74	5043	26.4
D5	D3X	Volatile Oil (B_{ob} = 2.3 and R_S = 407 Sm^3/Sm^3)	EOS6	670	1134	20.3	399	1471	25.4	4	4282	30.9
	D3		BO6	678	1121	20.2	401	1459	25.3	24	1386	31.0
D6	D4X	Medium Rich Gas Condensate ($V_{ro\,Max}$ = 12% and r_s = 0.00066 Sm^3/Sm^3)	EOS6	336	2744	23.3	197	3745	30.2	80	5159	38.5
	D4		BO6	337	2733	23.3	199	3711	30.1	83	4957	38.7
D7	D5X	Slightly Volatile Oil (B_{ob} = 1.8 and R_S = 256 Sm^3/Sm^3)	EOS6	815	806	20.0	477	1034	24.9	14	805	28.8
	D5		BO6	810	812	19.9	472	1043	24.7	16	973	28.6
Initial Fluid, Variable												
D8	E2A1X	Mainly Oil and some GC with fluid gradient as in bottom layer	EOS6	432	1982	24.0	216	3123	28.2	66	4882	32.6
	E2A1		BO6	438	1965	24.8	219	3097	29.1	73	4753	33.4
D9	E2A2X	Gas Condensate and Oil with fluid gradient as in middle layer	EOS6	349	2558	20.3	190	3709	24.7	45	5266	29.5
	E2A2		BO6	352	2550	20.6	191	3687	25.0	44	5101	29.8
D10	E2A3X	Only Gas Condensate fluid gradient as in top layer.	EOS6	223	1900	9.3	165	2390	13.2	86	3405	19.4
	E2A3		BO6	210	1835	8.9	158	2270	12.6	87	3203	18.6
D11	E2A3_10X	Only Gas Condensate fluid gradient as in top layer (k=50 md)	EOS6	329	2766	20.4	186	3870	25.5	61	5310	31.4
	E2A3_10		BO6	330	2765	20.8	187	3862	25.9	57	5271	31.8
Permeability Variations												
D12	D3F2X	Volatile Oil, Permeability High-Top	EOS6	256	3187	10.7	134	4470	12.5	0	5397	14.2
	D3F2		BO6	245	3324	10.5	128	4631	12.3	0	5243	13.8
D13	D3F3X	Volatile Oil, Permeability High-Middle	EOS6	255	3205	12.4	133	4514	14.2	0	5452	15.9
	D3F3		BO6	247	3302	12.4	130	4617	14.1	0	5807	15.7
Saturated GOC												
D14	D3M2X	Volatile Oil, constant oil and gas composition	EOS6	340	2526	19.8	185	3646	24.0	72	5031	28.7
	D3M2_CCE		BO6	316	2756	19.2	170	4003	23.1	65	5572	27.5
	D3M2_DLE		BO6	301	2899	18.9	158	4324	22.6	57	6051	26.6
	D3M2_MIX		BO6	344	2527	19.8	190	3586	24.1	74	4888	29.0
D15	D3M2E2X	Oil and Gas gradient	EOS6	352	2482	25.5	196	3545	30.7	74	5180	36.7
	D3M2E2_CCE		BO6	332	2651	24.8	182	3844	29.7	69	5518	35.3
	D3M2E2_DLE		BO6	317	2783	24.4	169	4142	29.1	63	6016	34.2
	D3M2E2_MIX		BO6	360	2436	25.6	202	3451	31.1	79	4845	37.4
D16	D3M2E2X_3W_RATE	Oil and Gas gradient (3 wells- top, middle & bottom)	EOS6	362	2392	22.7	203	3404	28.2	80	4809	34.5
			BO6	370	2347	23.2	208	3323	28.9	82	4660	35.4
		Structurally bottom well (P5010)	EOS6	162	1726	-	84	2672	-	30	4136	-
			BO6	155	1823	-	83	2739	-	31	4015	-
		Structurally middle well (P2505)	EOS6	102	2871	-	60	3875	-	25	5215	-
			BO6	108	2706	-	63	3687	-	25	5052	-
		Structurally top well (P0101)	EOS6	98	2993	-	59	3970	-	25	5235	-
			BO6	107	2743	-	63	3722	-	25	5061	-

Table 9— Simulation Cases and Performance — Injection

Case Name	File Name	Case Description	Model	Reservoir Performance								
				AFTER 5 YEARS			AFTER 10 YEARS			AFTER 15 YEARS		
				FOPR Sm^3/d	FGOR Sm^3/Sm^3	RF_r %	FOPR Sm^3/d	FGOR Sm^3/Sm^3	RF_r %	FOPR Sm^3/d	FGOR Sm^3/Sm^3	RF_r %
I1	J2B2D1C3X	Near Critical Fluid, Lean Gas Injection	EOS22	863	1386	39.5	513	2443	59.5	264	4871	71.1
	J2B2D1X		EOS6	838	1437	39.2	511	2457	59.0	290	4427	71.3
Gas Condensate Reservoirs with Constant												
I2	J2B2D1X	Near Critical Fluid, Lean Gas Injection	EOS6	838	1437	39.2	511	2457	59.0	290	4427	71.3
	J2B2D1		BO6	1147	983	44.2	733	1625	72.6	316	4054	88.7
I3	J2B2D2X	Rich Gas Condensate, Lean Gas Injection	EOS6	776	1576	43.4	446	2859	68.2	217	6014	81.8
	J2B2D2		BO6	819	1477	44.7	494	2562	71.8	238	5535	86.8
I4	J2B2D4X	Medium Rich Gas Condensate, Lean Gas Injection	EOS6	493	2598	44.1	287	4568	69.1	123	10890	82.4
	J2B2D4		BO6	501	2554	44.1	298	4412	69.7	144	9315	84.2
I5	J2B2D1Z2X	Near Critical Fluid, Lean Gas Injection, gravity stable	EOS6	176	575	5.5	175	577	10.9	174	585	16.4
	J2B2D1Z2		BO6	175	576	5.5	174	579	10.9	172	586	16.3
I6	J2B2D2Z2X	Rich Gas Condensate, Lean Gas Injection, gravity stable	EOS6	129	870	5.5	129	874	10.9	128	880	16.4
	J2B2D2Z2		BO6	129	870	5.5	128	874	10.9	127	881	16.3
Oil Reservoirs with Constant Composition												
I7	J2B2D5X	Slightly Volatile oil (SVO), Lean Gas Injection	EOS6	955	1180	37.5	424	2891	49.6	277	4499	56.2
	J2B2D5	SVO, Lean Gas Injection, black-oil extrapolation by Ecl	BO6	1195	902	42.0	623	1888	57.5	509	2309	68.8
	J2B2D5Y2_A	SVO, Lean Gas Injection, black-oil extrapolation by method A	BO6	1181	910	40.9	631	1846	56.6	513	2272	67.7
	J2B2D5Y2_B	SVO, Lean Gas Injection, black-oil extrapolation by method B	BO6	1141	950	40.8	619	1889	56.0	519	2244	67.2
	J2B2D5Y2_C	SVO, Lean Gas Injection, black-oil extrapolation by method C	BO6	1172	908	40.9	606	1912	56.2	499	2313	66.9
I8	J2B2D5T2X	SVO, Lean Gas Injection	EOS6	1039	1107	37.6	483	2656	51.2	354	3704	58.9
	J2B2D5T2Y2_B	SVO, (with vaporization and swelling)	BO6	1125	1014	40.2	666	1875	55.8	552	2299	68.0
	J2B2D5T2Y2_B_PVDG	SVO (no vaporization)	BO6	1295	828	48.2	252	5177	59.4	117	11471	62.7
	J2B2D5T2Y2_B_PVDG_DRSDT	SVO, (no vaporization and no swelling)	BO6	1171	934	46.9	253	5156	57.4	121	11052	60.8
I9	J2B2D6T2X	Low GOR oil, Lean Gas Injection	EOS6	2742	269	37.0	1231	894	59.4	461	2781	68.6
	J2B2D6T2Y2_A	Low-GOR oil, LG injection, black-oil extrapolation by method A	BO6	2171	394	33.2	1239	888	55.1	809	1489	67.9
	J2B2D6T2Y2_B	Low-GOR oil, LG injection, black-oil extrapolation by method B	BO6	2246	371	33.7	1202	920	55.0	767	1581	67.2
	J2B2D6T2Y2_C	Low-GOR oil, LG injection, black-oil extrapolation by method C	BO6	2227	386	33.0	1256	847	55.5	818	1405	68.3
I10	J2B2D6T2X_200	Low GOR oil, Lean Gas Injection (Initial Pr = 200 bara)	EOS6	2351	62	25.3	904	681	49.1	309	2200	56.2
	J2B2D6T2Y2_A_200	Low-GOR oil, LG injection, black-oil extrapolation by method A	BO6	2394	65	25.9	1027	594	50.3	411	1661	59.2
	J2B2D6T2Y2_B_200	Low-GOR oil, LG injection, black-oil extrapolation by method B	BO6	2210	79	25.2	969	627	47.9	424	1591	56.7
	J2B2D6T2Y2_C_200	Low-GOR oil, LG injection, black-oil extrapolation by method C	BO6	2340	65	25.7	1063	521	51.0	415	1446	60.0
I11	J2B2D6T2X	Low-GOR oil, Lean Gas, Injection	EOS6	2742	269	37.0	1231	894	59.4	461	2781	68.6
	J2B2D6T2Y2_B	Low-GOR oil (with vaporization and swelling)	BO6	2246	371	33.7	1202	920	55.0	767	1581	67.2
	J2B2D6T2Y2_B_PVDG	Low-GOR oil (no vaporization)	BO6	2489	307	40.9	996	1135	61.4	383	3332	69.7
	J2B2D6T2Y2_B_PVDG_DRSDT	Low-GOR oil (no vaporization and no swelling)	BO6	1214	837	28.2	604	1967	38.9	387	3238	45.1
I12	J4B2D5X	SVO, Injection C1N2	EOS6	872	1312	34.8	436	2807	46.4	436	2807	46.4
	J4B2D5Y2_B	SVO, Injection C1N2, black-oil extrapolation by method B	BO6	1138	940	40.8	587	1950	55.7	587	1950	55.7
	J4B2D5Y2_C	SVO, Injection C1N2, black-oil extrapolation by method C	BO6	1155	916	40.7	577	1973	55.6	577	1973	55.6
Compositional Gradient (Reservoirs with Undersaturated GOC)												
I13	J2B2E2A2X	Fluid gradient as in middle layer, Injection of LG	EOS6	480	2648	38.5	268	4850	53.8	168	7834	62.9
	J2B2E2A2		BO6	509	2489	39.5	301	4317	56.2	198	6628	66.7
Permeability Variation (Near Critical Fluid)												
I14	J2B2D1F2X	Near Critical Fluid, High Perm at Top, Injection Lean Gas	EOS6	584	2137	30.5	305	4223	43.3	157	8327	50.3
	J2B2D1F2		BO6	620	2005	31.7	371	3441	46.7	251	5140	56.2
I15	J2B2D1F3X	Near Critical Fluid ,High Perm at Middle, Injection Lean Gas	EOS6	706	1743	35.5	203	6426	47.6	153	8536	52.7
	J2B2D1F3		BO6	799	1514	40.6	268	4843	54.6	155	8477	60.6
Undersaturated Oil Reservoirs												
I16	J2B3D3X	Volatile Oil, Inject (lean gas) 50% of produced gas	EOS6	740	916	24.9	5	2336	26.8	0	0	26.8
	J2B3D3		BO6	728	770	25.1	23	798	27.2	0	0	27.2
I17	J2B4D3X	Volatile Oil, Inject (lean gas) 80% of produced gas	EOS6	885	1108	25.8	453	2142	31.9	1	2944	35.4
	J2B4D3		BO6	1097	853	27.1	589	1594	35.0	0	0	37.9
I18	J2B5D3X	Volatile Oil, Inject (lean Gas) all produced gas	EOS6	883	1190	25.7	553	1949	32.4	273	3968	42.3
	J2B5D3		BO6	1149	860	27.7	676	1532	36.3	397	2594	48.6
Oil Reservoir with Gas Injection in Gas Cap												
I19	J2B3E2A2X	Layer 2 gradient, Inject (lean gas) 50% of produced gas	EOS6	447	2333	23.1	120	2979	27.6	3	2498	29.1
	J2B3E2A2		BO6	488	2137	24.7	128	2599	29.8	0	0	31.1
I20	J2B4E2A2X	Layer 2 gradient, Inject (lean gas) 80% of produced gas	EOS6	502	2268	24.4	319	3434	31.2	98	6300	40.1
	J2B4E2A2		BO6	557	2025	26.6	374	2912	34.3	118	4732	45.1
I21	J2B5E2A2X	Layer 2 gradient, Inject (lean Gas) all produced gas	EOS6	553	2174	25.5	393	3080	33.3	231	5225	45.9
	J2B5E2A2		BO6	647	1822	28.3	462	2575	37.5	270	4394	52.4
Permeability Variation												
I22	J2B5E2A2F2X	Layer 2 gradient, Inject all produced gas (LG), highest k at top	EOS6	511	2382	22.8	354	3464	30.0	198	6177	41.1
	J2B5E2A2F2		BO6	584	2042	25.1	400	3014	33.2	221	5480	45.6
I23	J2B5D3F2X	Volatile Oil, Inject all produced gas (LG), highest K at top	EOS6	558	2078	16.6	396	2940	21.2	238	4848	28.7
	J2B5D3F2		BO6	605	1912	17.0	441	2622	22.1	269	4231	30.6

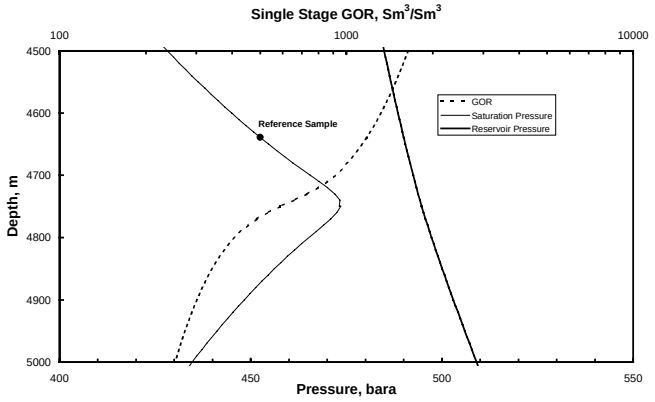

Fig. 1 — GOR, reservoir and saturation pressure variation with depth.

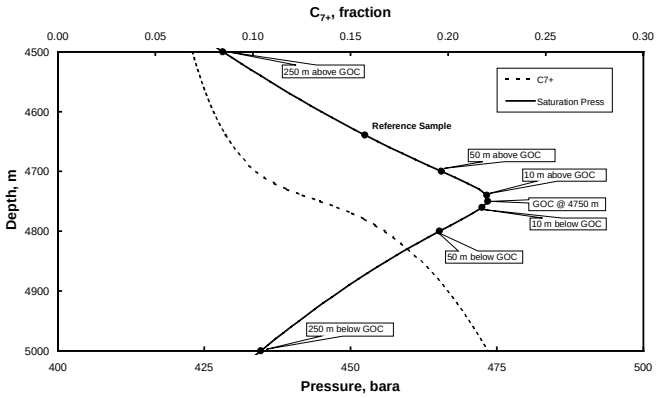

Fig. 2 — C_{7+} variation with depth and different feed locations.

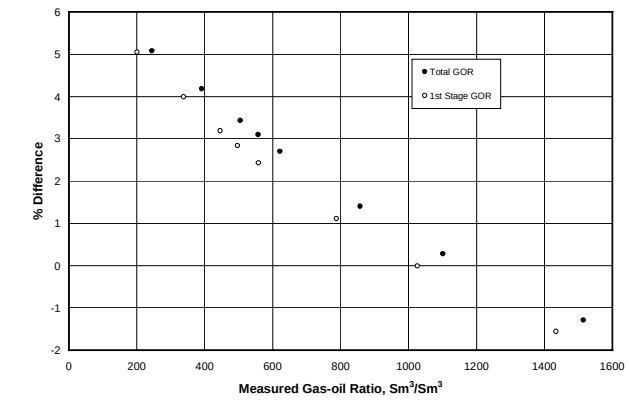

Fig. 3 — Difference in separator gas-oil ratio - EOS22 vs. EOS6 (separator experiment).

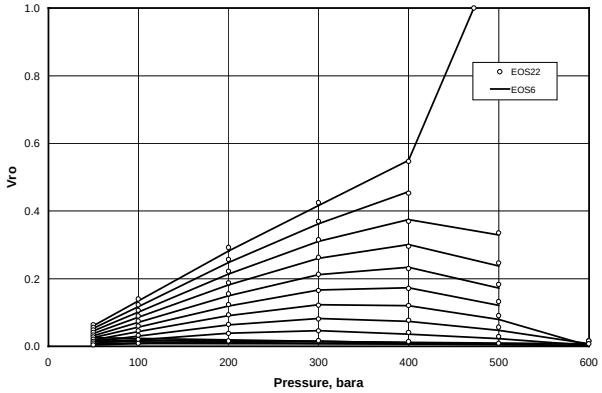

Fig. 4 — Relative oil volume comparison - EOS22 vs. EOS6 : rich gas injection in oil sample (multicontact swelling experiment).

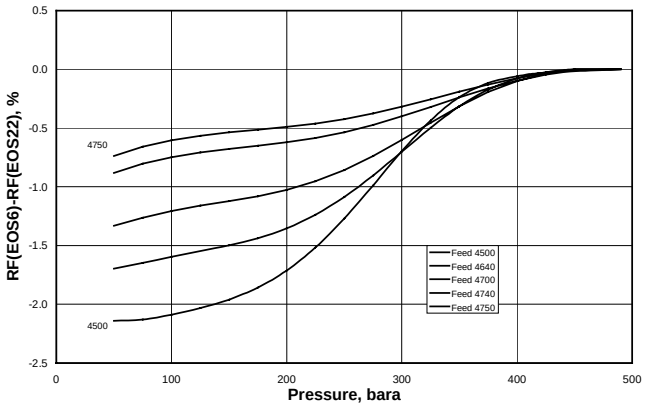

Fig. 5 — Difference in oil recovery - EOS22 vs. EOS6 based on CVD data.

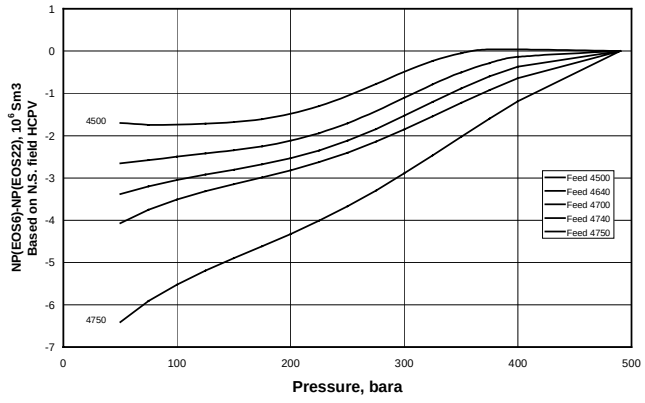

Fig. 6 — Difference in total oil production - EOS22 vs. EOS6 based on CVD data.

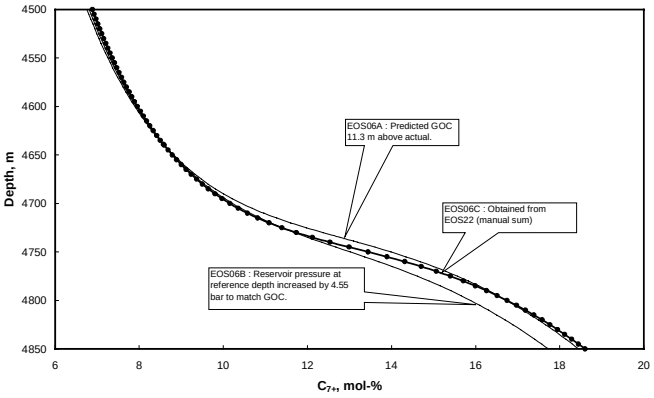

Fig. 7 — C_{7+} composition variation with depth under different initialization methods.

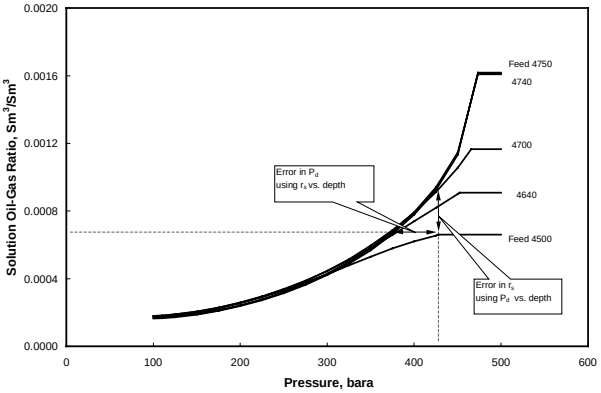

Fig. 10 — Initializing black-oil model — (a) solution OGR vs. depth (b) saturation pressure vs. depth

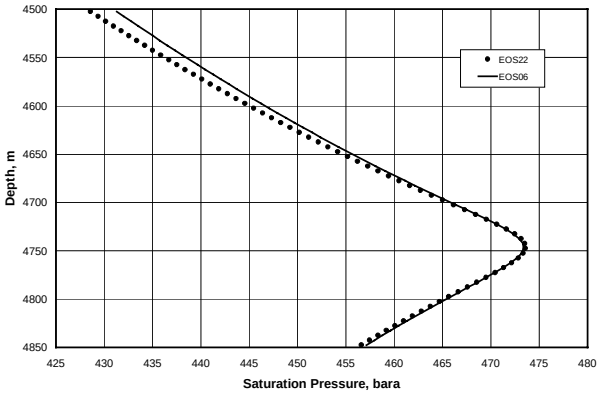

Fig. 8 — Saturation pressure with depth (EOS22 vs. EOS6).

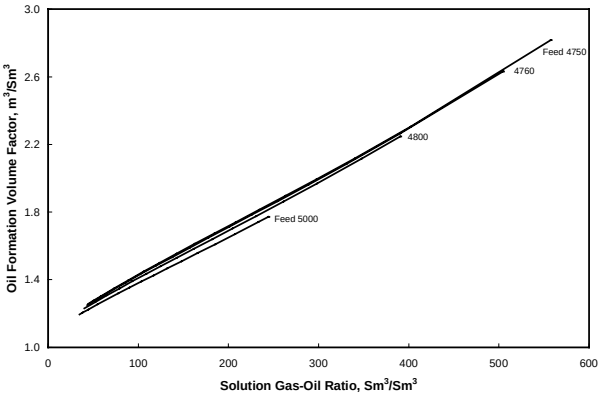

Fig. 11 — Oil formation volume factor versus solution gas-oil ratio for fluids from different locations.

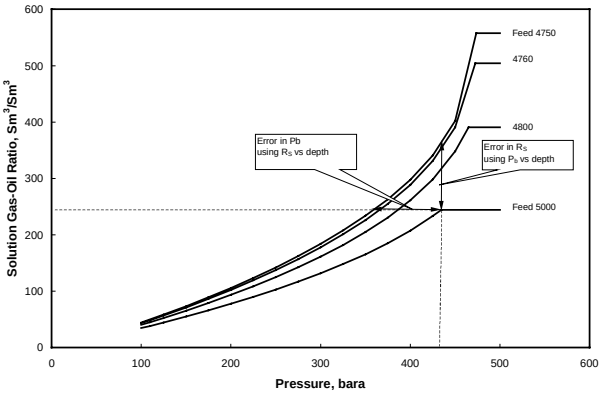

Fig. 9 — Initializing black-oil model — (a) solution GOR vs. depth (b) saturation pressure vs. depth

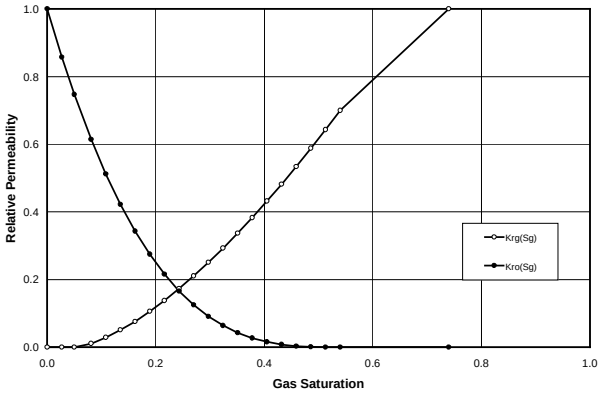

Fig. 12 — Oil and gas relative permeabilities.

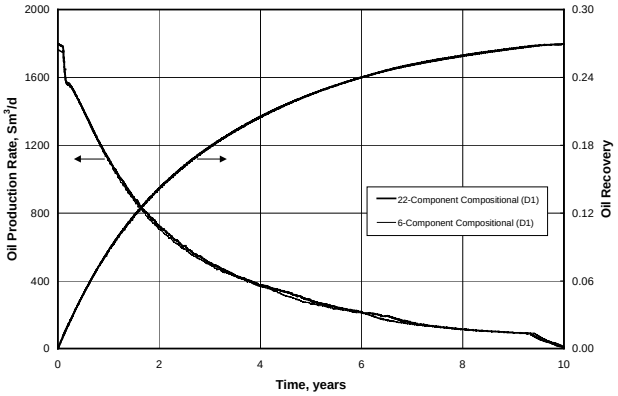

Fig. 13 — Depletion Case - EOS22 vs. EOS6 (near critical fluid with constant composition).

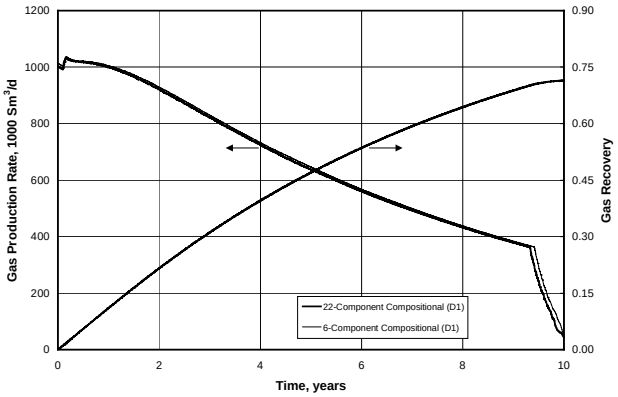

Fig. 14 — Depletion Case - EOS22 vs. EOS6 (near critical fluid with constant composition).

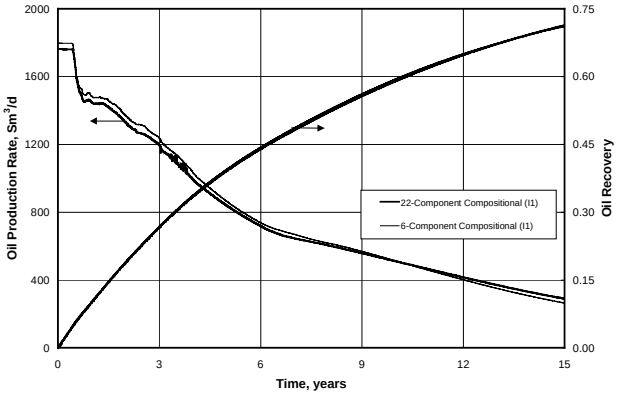

Fig. 15 — Injection Case - EOS22 vs. EOS6 (near critical fluid with constant composition).

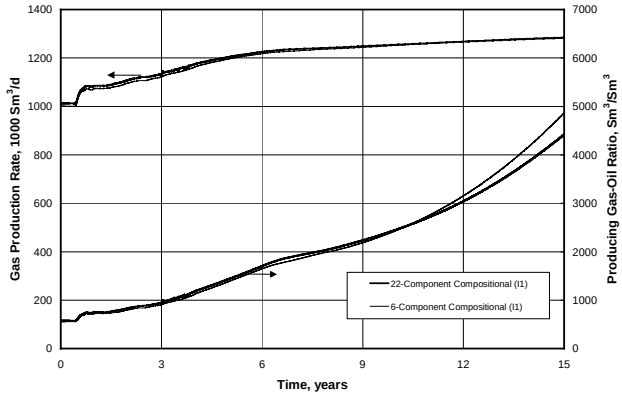

Fig. 16 — Injection Case - EOS22 vs. EOS6 (near critical fluid with constant composition).

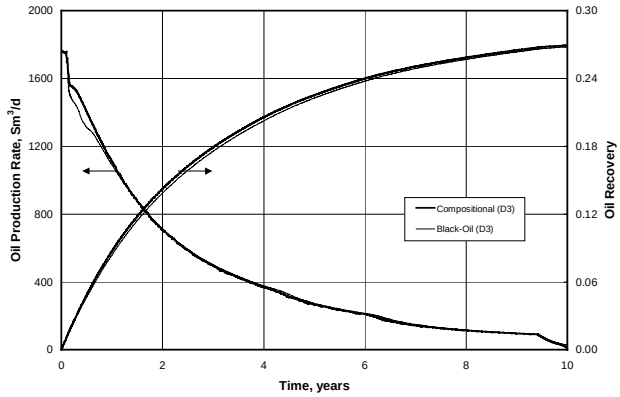

Fig. 17 — Depletion Case - Near critical fluid with constant composition; EOS6.

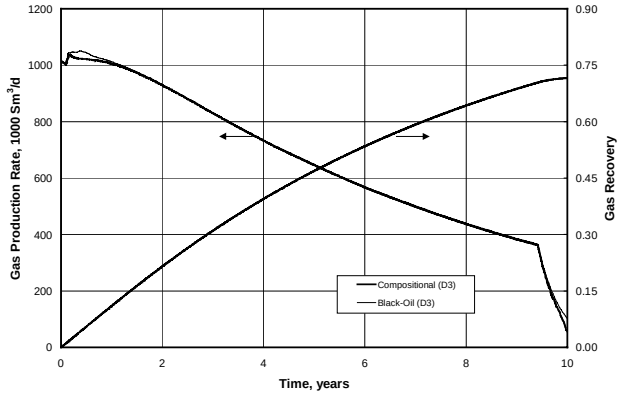

Fig. 18 — Depletion Case - Near critical fluid with constant composition; EOS6.

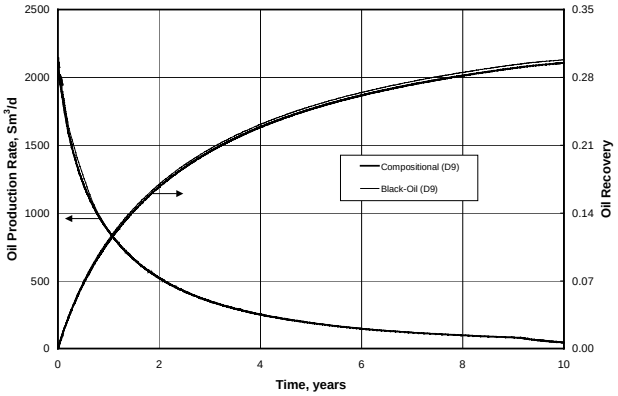

Fig. 19 — Depletion Case - Reservoir with Compositional Gradient; EOS6.

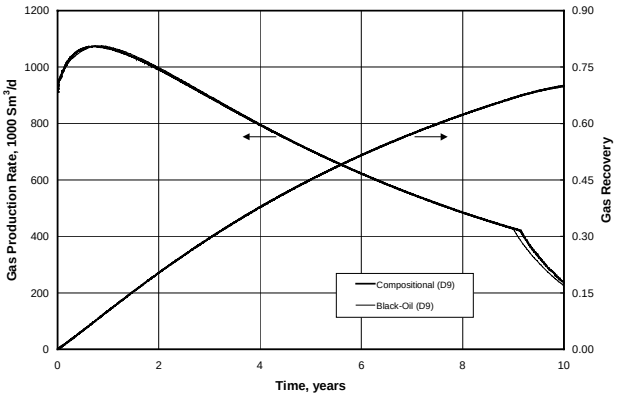

Fig. 20 — Depletion Case - Reservoir with compositional gradient; EOS6.

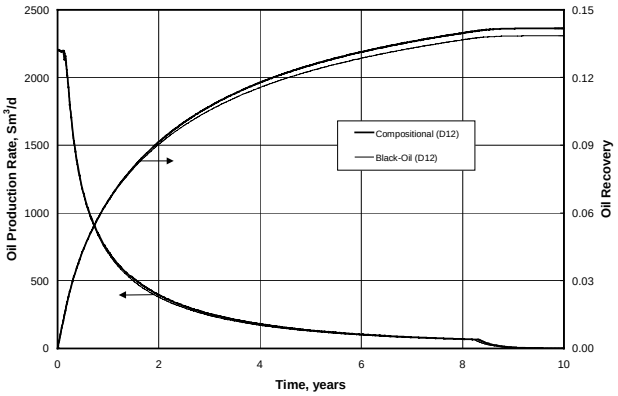

Fig. 21 — Depletion Case - Volatile oil reservoir with constant composition and highest permeability at the top; EOS6.

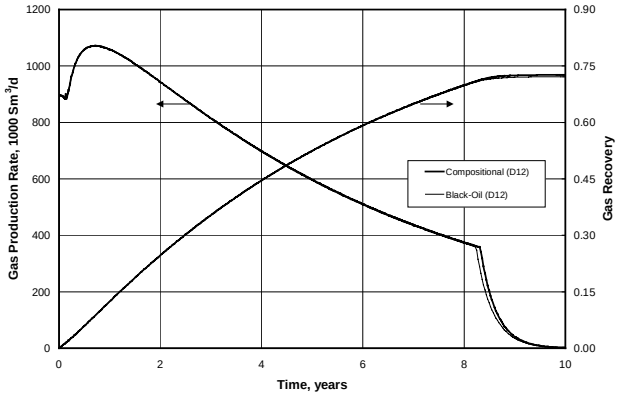

Fig. 22 — Depletion Case - Volatile oil reservoir with constant composition and highest permeability at the top; EOS6.

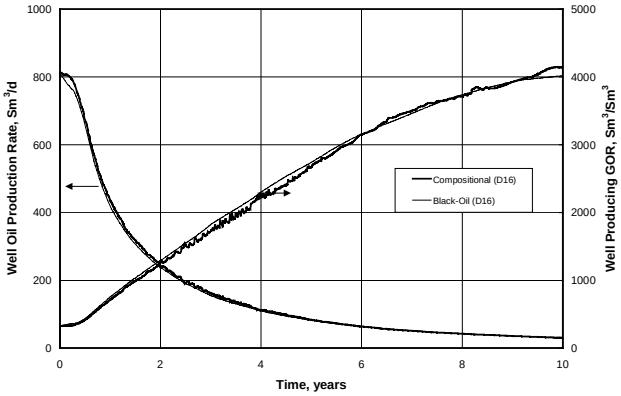

Fig. 23 — Depletion Case - Reservoir with compositional gradient with saturated GOC (structurally low well); EOS6.

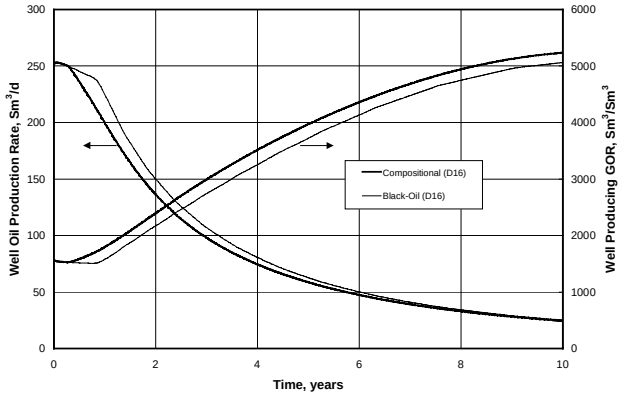

Fig. 24 — Depletion Case - reservoir with compositional gradient with saturated GOC (structurally high well); EOS6.

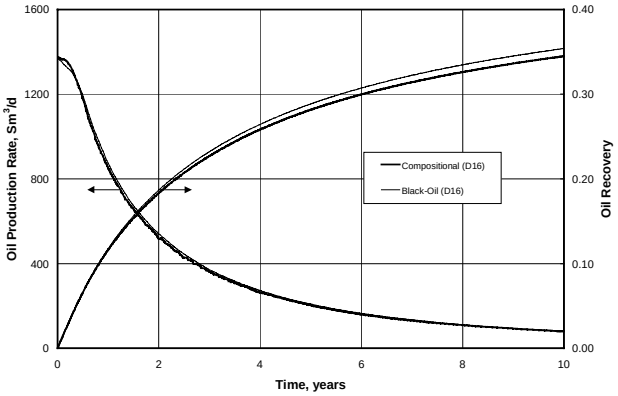

Fig. 25 — Depletion Case - Reservoir with compositional gradient with saturated GOC (total field – all three wells); EOS6.

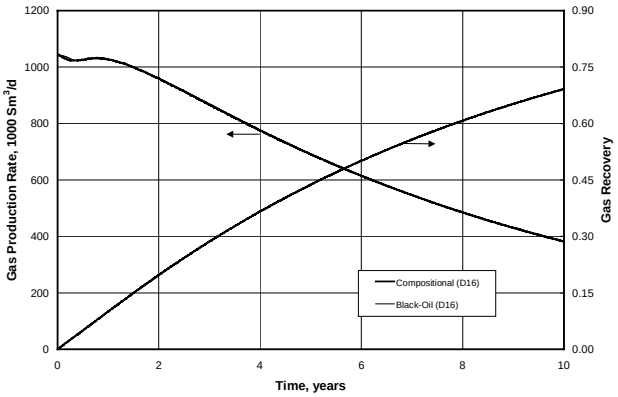

Fig. 26 — Depletion Case - reservoir with compositional gradient with saturated GOC (total field – all three wells); EOS6.

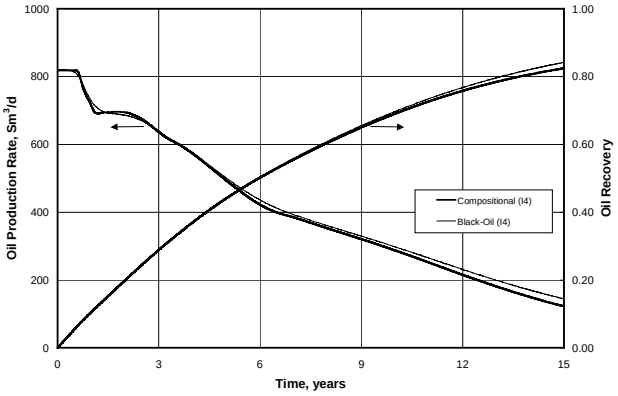

Fig. 27 — Injection Case - Medium rich gas condensate with constant composition; EOS6.

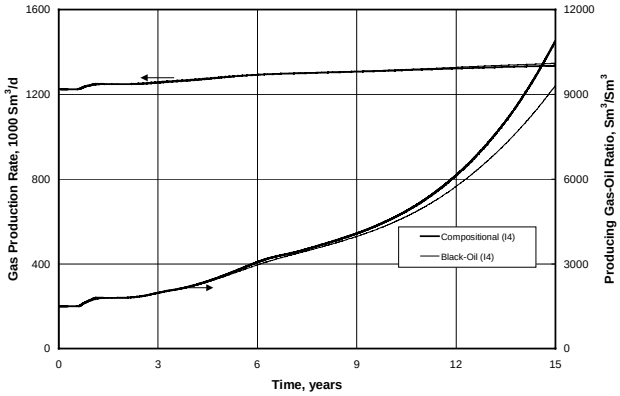

Fig. 28 — Injection Case - Medium rich gas condensate with constant composition; EOS6.

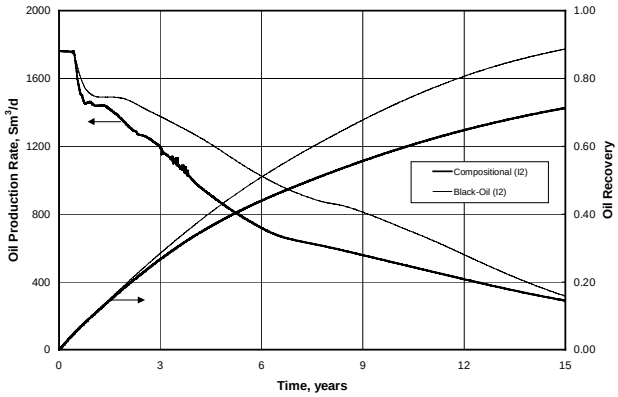

Fig. 29 — Injection Case - Near critical fluid with constant composition; EOS6.

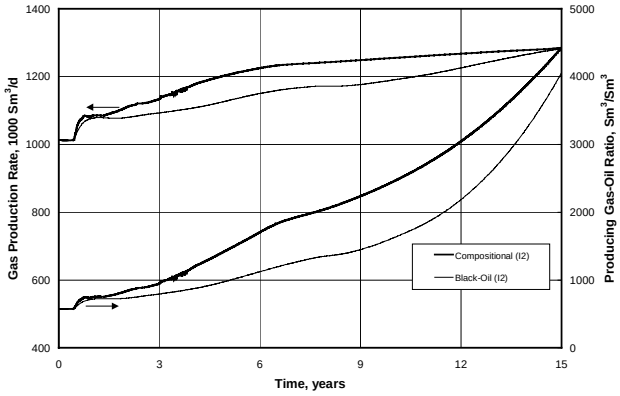

Fig. 30 — Injection Case - Near critical fluid with constant composition; EOS6.

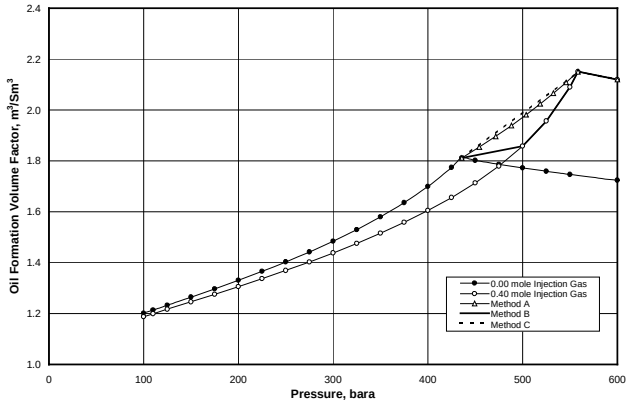

Fig. 31 — Modified BO PVT table (oil formation volume factor) for lean gas injection in slightly volatile oil.

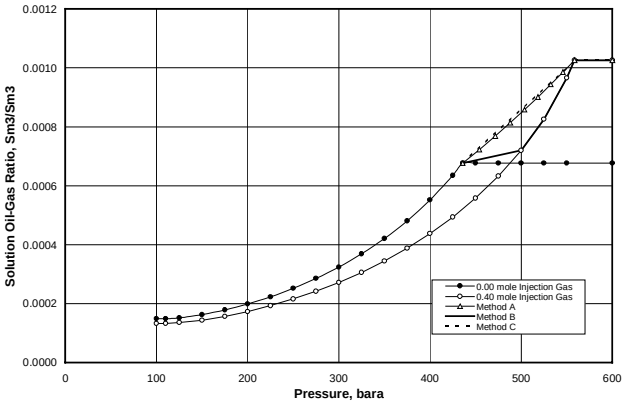

Fig. 34 — Modified BO PVT table (oil-gas ratio) for lean gas injection in slightly volatile oil.

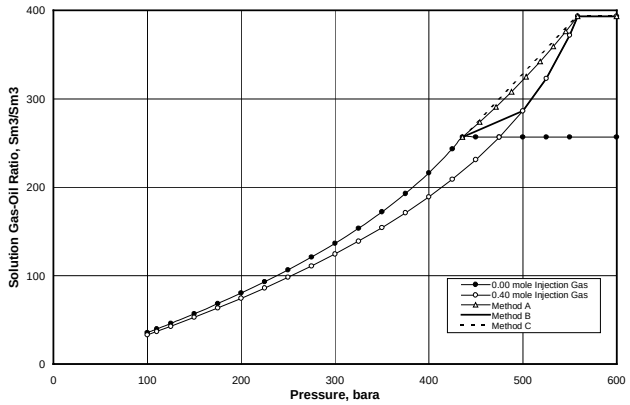

Fig. 32 — Modified BO PVT table (solution gas-oil ratio) for lean gas injection in slightly volatile oil.

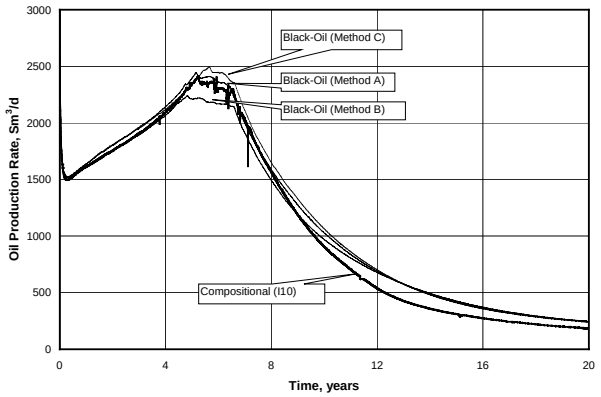

Fig. 35 — Injection Case - Low GOR (50 Sm^3/Sm^3) oil with constant composition. Average reservoir pressure P_R= 200 bara and saturation pressure P_b= 135 bara; EOS6.

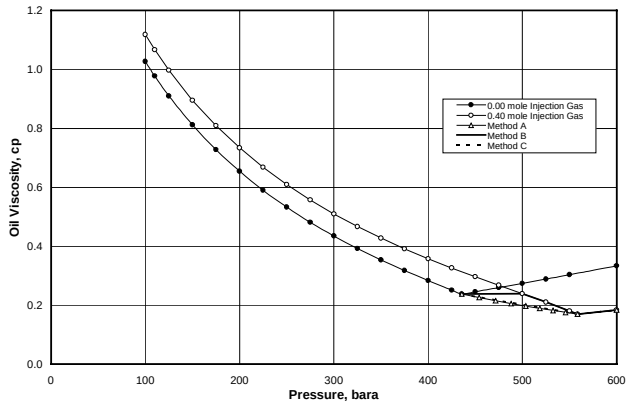

Fig. 33 — Modified BO PVT table (oil viscosity) for lean gas injection in slightly volatile oil.

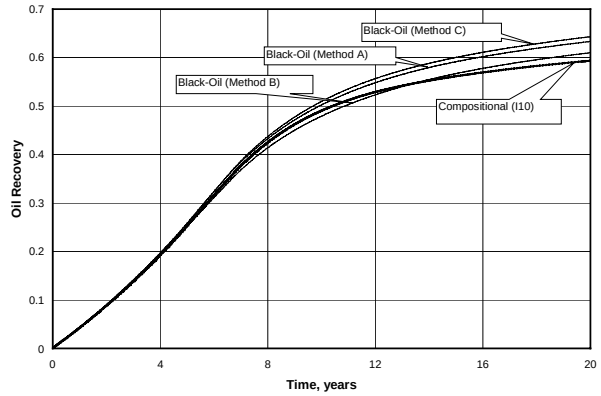

Fig. 36 — Injection Case - Low GOR (50 Sm^3/Sm^3) oil with constant composition. Average reservoir pressure P_R= 200 bara and saturation pressure P_b= 135 bara; EOS6.

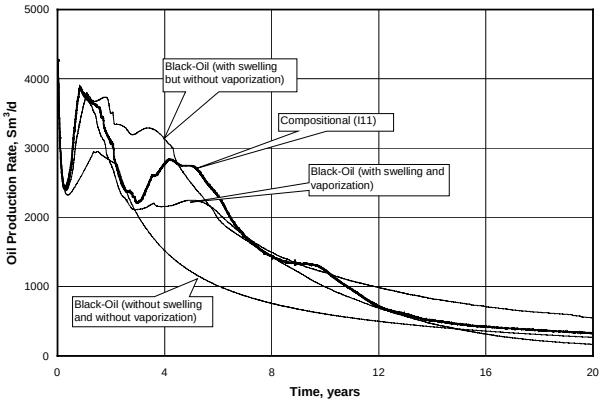

Fig. 37 — Injection Case - Low GOR oil with constant composition (with and without —swelling and vaporization). Average reservoir pressure P_R= 500 bara and saturation pressure P_b= 135 bara; EOS6.

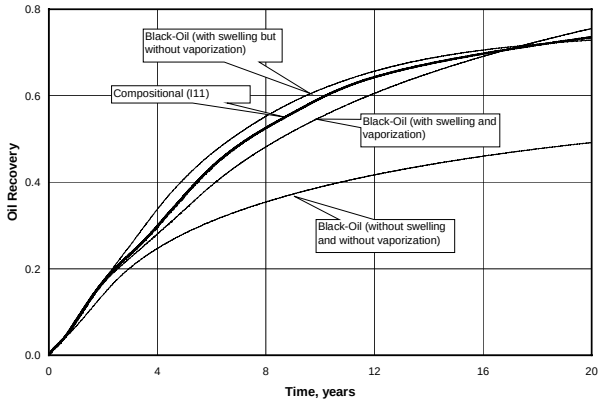

Fig. 38 — Injection Case - Low GOR Oil with constant composition (with and without —swelling and vaporization). Average reservoir pressure P_R= 500 bara and saturation pressure P_b= 135 bara; EOS6.

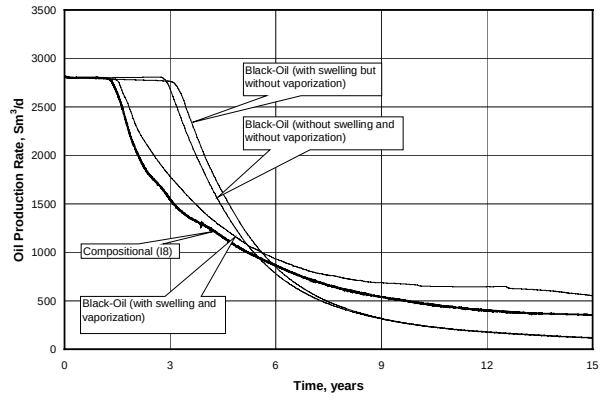

Fig. 39 — Injection Case - Slightly volatile oil with constant composition (with and without —swelling and vaporization); EOS6.

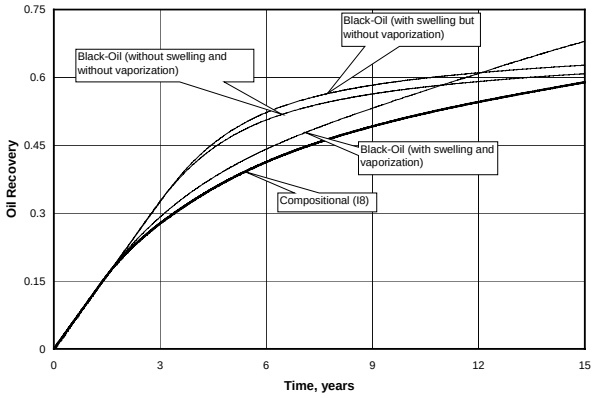

Fig. 40 — Injection Case - Slightly volatile oil with constant composition (with and without —swelling and vaporization) ; EOS6.

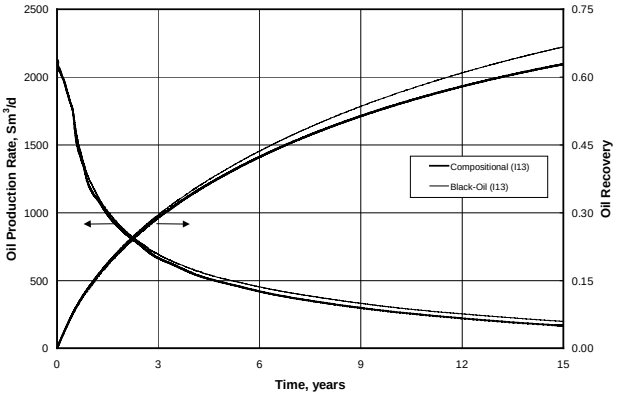

Fig. 41 — Injection Case - Reservoir with compositional gradient; EOS6.

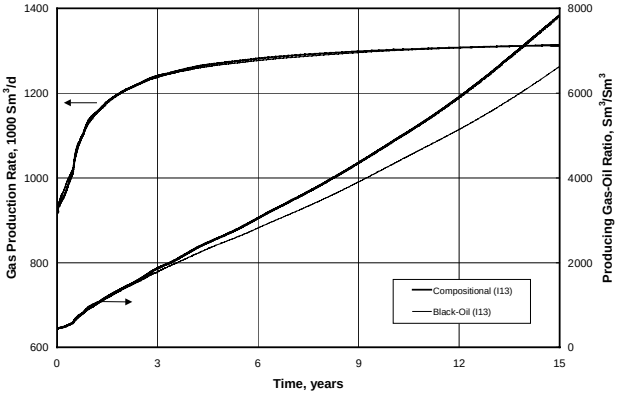

Fig. 42 — Injection Case - Reservoir with compositional gradient; EOS6.

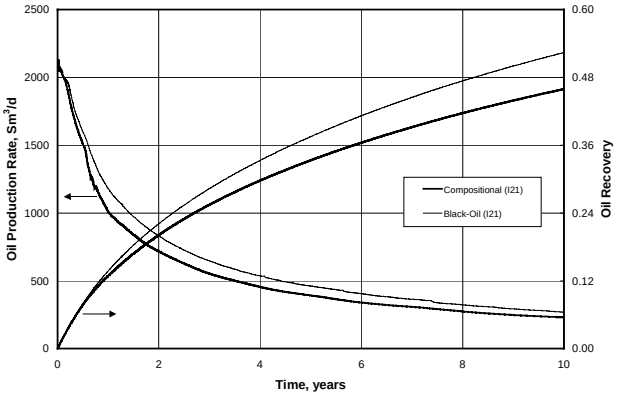

Fig. 43 — Injection Case - Reservoir with compositional gradient and 100% of the surface produced gas reinjected; EOS6.

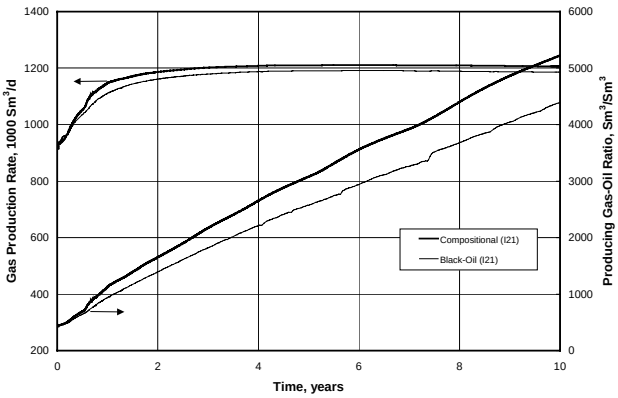

Fig. 44 — Injection Case - Reservoir with compositional gradient and 100% of the surface produced gas reinjected; EOS6.